

On the critical cluster in the two-dimensional Ising model: Computer-assisted exact results

Vitaly A. Shneidman and Gelu M. Nita

Department of Physics, New Jersey Institute of Technology, Newark, New Jersey 07102

(Received 13 July 2004; accepted 15 September 2004)

For a nearest-neighbor Ising model on a square lattice all cluster configurations with 17 or fewer spins are identified. In neglect of cluster-cluster interactions, critical sizes and barriers to nucleation are obtained as functions of temperature and magnetic field for two alternative definitions of a “critical cluster.” © 2004 American Institute of Physics. [DOI: 10.1063/1.1814080]

I. INTRODUCTION

From the early days of classical nucleation theory¹ (CNT) it was clear that one of its main restrictions comes from treating the nucleus as a macroscopic particle. In reality, a typical critical nucleus contains only a handful of monomers $n_* \sim 10^1$, and recently several diverse experimental situations where the structure of a nucleus is qualitatively different from that of the stable phase were identified.^{2,3}

Another, even more serious limitation of CNT, already noted by Farkas in 1927 (Ref. 1) (see also Ref. 4) comes from the fact that there is a macroscopically undetermined factor in the equilibrium distribution of clusters $f_n \sim \exp\{-W_n/T\}$ (Boltzmann constant is taken as 1). Even if the critical nucleus is large, $n_* \gg 1$, evaluation of the prefactor requires $n \sim 1$, where the minimal work to form an n -monomer cluster, W_n hardly can be any close to the bulk, “surface plus volume,” value.

On the other hand, the very fact that the n is relatively small, makes a nucleus an attractive object for computer studies. For example, powerful equilibrium Monte Carlo (MC) tools to describe a critical nucleus are being developed, e.g., Ref. 5. Dynamic MC approaches allow one to study the entire nucleation process^{6–13} for lattice systems of the Ising type. For such systems computers also provide a remarkable possibility of an exact description of clusters, in certain cases enabling crucial tests of more intuitive descriptions of nucleation or, on a more practical level, allowing one to test the MC methods (which, typically do require an independent verification due to the extreme rarity of the nucleation events⁶). One also can hope to preserve the attractive features of CNT by using bulk values of W_n but employing the exact data to adjust the prefactor in the equilibrium distribution, thus substantially improving the accuracy.⁶

The two-dimensional Ising model with external field H (“supersaturation” in the equivalent lattice-gas terminology) provides the simplest, yet nontrivial example of a nucleating system. Here the definition of a “cluster” is straightforward for not too high temperatures, while availability of exact expressions for the interfacial tension allows one to specify the bulk limit of CNT (see Refs. 6 and 14 for the square and triangular lattice, respectively, and references therein). Exact finite-size expressions for the critical size and the barrier W_* are also available in the limit $T \rightarrow 0$ ¹⁵ for arbitrary values of

the field. Also, at $T=0$ the preexponential of the nucleation rate can be obtained both for strong¹⁶ and arbitrary fields^{17,18} for several Glauber-type dynamics. Moreover, even at finite (albeit small) T the full expression for the nucleation rate, including the preexponential, can be derived analytically [small T , arbitrary H (Refs. 18 and 19)] or using symbolic computations [higher T , moderate-to-high H (Refs. 20 and 21)]. Non-Glauber dynamics also was considered recently for strong fields.^{22,23}

The general difficulty in considering finite temperature and weak fields is that an enormous number of cluster configurations can contribute to nucleation. Thus, in the full dynamic problem the nucleation rate can be evaluated only for rather modest values of n_* , currently ≤ 7 [which corresponds to $H \geq 1$ if $T \rightarrow 0$ (Ref. 15)]. Already for the next zero- T value of $n_* = 13$ the full dynamics of cluster-cluster transitions is too rich and either some “pruning” of the nucleation paths is required in the symbolic analytical treatment,²¹ or numerical approaches are to be used.⁷

In the present study exact low-temperature equilibrium cluster populations at $n \leq 17$ are obtained with a breakdown by energies (numbers of bonds). This can be of independent interest, but will also permit to gain some insight into the structure of n_* and W_* at finite temperatures and weak fields. Larger values of n compared to Refs. 20 and 21 are achieved mostly at the expense of disregarding the dynamics of cluster-cluster transitions, increasing the number of configurations which can be identified. Fundamental difficulties in rigorously defining n_* and W_* (which, within the CNT context are asymptotic, rather than exact quantities) are also highlighted. Once a definition of those quantities is specified, however, their H, T map can be constructed with the situation being very rich compared to the zero- T limit of Ref. 15.

II. THE MODEL

Consider the standard Ising model with the total energy given by

$$\mathcal{H} = -J \sum_{nn} \sigma_i \sigma_k - H \sum_i \sigma_i. \quad (1)$$

Here $J > 0$ is the interaction energy between two neighboring spins, $\sigma = \pm 1$ is the spin variable (and nn indicates summation over all nearest-neighbor pairs). The system is assumed

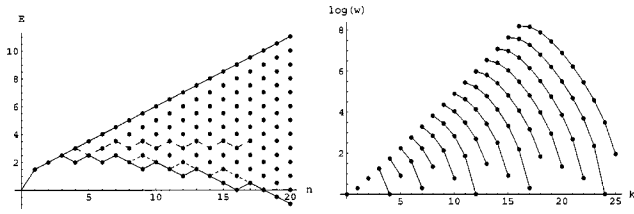


FIG. 1. Cluster energies E_n^k (left, in units of $4J$) and numbers of configurations w_n^k (right) for different numbers of spins n and bonds k . Values of E_n^k on the left are from Eq. (3) with $h=0.25$. The upper bound (straight line) and the lower bound (cusped line) correspond to $k=k_{\min}(n)$ and $k=k^{\max}(n)$, respectively. Degenerations of each state for $n \leq 17$ are given in the right part of figure (and in Table I) with solid lines connecting configurations with identical number of spins $n=k_{\min}+1$. Dashed lines in the left figure show the path corresponding to W_{\min}^n for $T=1J$ (lower line) and $T=2J$ (upper line), respectively.

to be metastable, i.e., prepared with all spins originally pointing in one direction (down), while the external field $H > 0$ prescribes an “up” orientation. Some standard spin flip dynamics should be kept in mind, although specification of the dynamics will not be required for most of the present study, as long as the detailed balance is satisfied.

A well-defined metastable state will persist for an exponentially long time, except for formation of isolated clusters containing n spins, k nearest neighbor pairs (bonds), and a variety of shapes. The energies of formation, i.e., the difference in \mathcal{H} once a given cluster is formed, are given by

$$E_n^k = 2JP_n^k - 2nH \quad (2)$$

with P_n^k being the perimeter of a cluster. Or, using a simple geometric relation $P_n^k = 4n - 2k$ (see Ref. 18) one has

$$E_n^k(h) = 8Jn(1-h) - 4Jk, \quad h = H/4J. \quad (3)$$

The minimal number of bonds for a given n corresponds to a linear chain with

$$k_{\min}(n) = n - 1. \quad (4)$$

Evaluation of the maximum number of bonds $k^{\max}(n)$ is slightly more elaborate,¹⁸ and depends on the position of n

relative to the closest perfect square. If one defines $m = [\sqrt{n}]$ (with $[x]$ being the largest integer not to exceed x), then

$$k^{\max}(n) = \begin{cases} 2(n-m), & n = m^2 \\ 2(n-m) - 1, & m^2 + 1 \leq n \leq m^2 + m \\ 2(n-m-1), & m^2 + m + 1 \leq n < (m+1)^2. \end{cases} \quad (5)$$

A typical arrangement of available energies is shown in the left Fig. 1. The points shift in the vertical direction with changing field; the upper line becomes horizontal for $h = 1/2$. At $h > 1/2$ one still can discuss conventional nucleation (with $n=1$ corresponding to the critical cluster at $1/2 < h < 1$), but subsequent growth of nuclei will be different since the interface becomes unstable.²⁴ In what follows, however, we focus on $h \leq 1/2$.

Once the energies are known, the number densities (quasi-equilibrium distributions) of noninteracting clusters can be determined as

$$f_n^k(h, T) = w_n^k \exp\{-E_n^k/T\}. \quad (6)$$

The values w_n^k represent the total number of configurations with given n and k . Evaluation of such numbers represent one of the primary goals of the present study.

III. RESULTS

A. Number of configurations

Results for the numbers w_n^k are given in Table I and are depicted in the right part of Fig. 1. For a fixed n the number of configurations monotonically decreases with k , with the rate of decrease being smaller near the smallest k .

Correctness of the numbers was verified by available tabulated data for small n ,²⁵ and by our earlier results obtained in the studies of the dynamic nucleation problem^{20,21} (where all cluster configurations could be identified for $n \leq 9$). To our knowledge, detailed data for larger n have not been reported previously, although cumulative data up to $n = 19$ are available²⁶ and could be used for verification. It is

TABLE I. Numbers w_n^k of distinct clusters with n spins and k nearest-neighbor bonds.

$n/k-n+1$	0	1	2	3	4	5	6	7	8	9
1	1									
2	2									
3	6									
4	18	1								
5	55	8								
6	174	40	2							
7	570	168	22							
8	1 908	677	134	6						
9	6 473	2 708	656	72	1					
10	22 202	10 724	3 008	482	30					
11	76 886	42 012	13 456	2 596	310	8				
12	268 852	163 494	58 742	13 034	2 086	151	2			
13	942 651	633 748	250 986	63 256	11 789	1 392	68			
14	3 329 608	2 448 760	1 056 608	297 262	62 396	9354	864	22		
15	11 817 582	9 436 252	4 401 192	1 359 512	317 722	5 4908	7 036	456	6	
16	42 120 340	36 285 432	18 173 796	6 095 764	1 563 218	30 3068	46 352	4 748	218	1
17	150 682 450	139 297 108	74 496 544	26 922 156	7 477 928	1 603 984	276 464	36 112	3 010	88

important to note that the computer effort involved in such computations increases rapidly with n since the number of configurations grows faster than an exponential, as described below. The available realization²⁷ of the standard algorithm²⁸ can be easily modified to get cluster breakdown by energies (and in combination with modern computer powers result up to $n \approx 20$ can be currently obtained²⁹). Nevertheless, the approach which was utilized in this work was closer to the one used in the dynamic problem;^{20,21} this allowed for additional cross testing, and details of the algorithm will be described elsewhere.³⁰

The total number of configurations for $n \leq 17$ can be approximated by

$$\sum_{k=k_{\min}(n)}^{k_{\max}(n)} w_n^k \approx \exp(a + bn + cn^2) \quad (7)$$

with $a = -1.731 \pm 0.50$, $b = 1.15 \pm 0.12$, and $c = 0.007 \pm 0.001$. Despite the small values of the positive coefficient c , its presence is essential for an accurate estimation. For example, a pure exponential interpolation suggested in Ref. 31 for $n \leq 10$ would underestimate the number of the largest configurations by more than two times if extrapolated to current values of n . Note, however, that the main intent of approximation (7) is to estimate the amount of computer resources required for a larger n . Otherwise, for physical applications one requires individual estimations for different energies and most of the higher-energy configurations [which give a major contribution to the sum (7)] will effectively not contribute for any reasonable temperature being far away from the nucleation path, as in the left part of Fig. 1.

From the right part of Fig. 1 one can see that as a function of k logarithms of the numbers of “open” configurations (with few bonds compared to the most compact cluster) increase approximately linearly. That is, one could draw near-straight lines (not shown in the figure) through configurations with k_{\min} bonds, with $k_{\min} + 1$ bonds, etc. This would allow one to make a crude estimation of w_n^k for the numbers of excited configurations at $n > 17$. On the other hand, the most compact configurations, which will not appear in those extrapolations (or the few first excited states which will be given inaccurately) can be obtained exactly since those states have a modest number of configurations even for large n . The latter approach was used, e.g., for the number of the most compact configurations of a 21-spin cluster, $w_{21}^{32} = 187$, which will be used below when estimating the critical size. The necessity of considering large n stems from the fact that small clusters might not reveal a general pattern either in the structure of the nucleation paths or in the field and temperature dependences of n_* . Indeed, at $T \rightarrow 0$ the critical number has the values $n_* = m^2 + m + 1$ with $m = 0, 1, 2, \dots$.¹⁵ The $n_* = 7$ is the first value where the nucleus can have excited states (and where the degeneracy of the lowest energy state leads to branching of the nucleation paths¹⁸). The next value $n_* = 13$ (smaller field) was already beyond the previous computational possibilities. The low-temperature boundary of the $n_* = 13$ domain is determined by $n_* = 17$ (see below), for which reason clusters with up to 17 spins were considered in the present study.

B. The critical cluster

Once the exact data for cluster distributions become available, the most delicate operation is the definition of the “critical cluster.” Note that the experimentally observable quantity is the nucleation rate I , and there is certain flexibility when the “barrier” and the “preexponential” are introduced.¹⁸ The same relates to the critical size. In constructing the formal definition one could wish to be able to recover the zero- T limit¹⁵ and at the same time to remain close to conventional wisdom based on CNT where the critical cluster either corresponds to the minimum (one-dimensional formulation) or the saddle point (multidimensional formulation) of the quasiequilibrium distribution. A kinetic definition of the critical cluster (which, within the CNT has an equal chance to grow or decay at long times) is used in Monte Carlo studies,⁸ but would require specification of the dynamics and will not be considered in the present work. (To avoid confusion with terminology, note that non-conventional kinetic definitions of a critical cluster were also suggested,³¹ with multiple values at a given pair of h, T , which also will not be considered here).

If n were the only argument of the quasiequilibrium distribution f_n , then unambiguously n_* would determine the minimum of this distribution. This is possible, however, only for $n_* \leq 3$ when clusters have no excited states (and the Becker-Döring type description of nucleation is accurate¹⁸). For larger clusters there is an additional parameter k (and many shapes with the same n and k), and there are more choices. Ideally, one would wish to identify a “saddle-point” configuration, but without specifying the dynamics (or, without introducing some formal metrics in the n, k space) this cannot be uniquely done even if the energy landscape is known. Since the present study is restricted to equilibrium properties, two alternatives will be discussed.

First, a “microscopic” definition can be introduced, which for a given n identifies a maximum f_n^k among all possible k , and then a minimum among such distributions is selected. This definition will be the closest to the saddle-point one. Alternatively, a thermodynamically averaged distribution can be constructed for each n , and then a similar minimum can be identified. (The latter case, most likely makes sense if there is an equilibration mechanism among different configurations with the same n , as in the Kawasaki dynamics, but it also allows one to come up with an upper bound for the nucleation rate in a more general case, as will be discussed later in the paper).

Let us introduce

$$W_n^k(h, T) = E_n^k(h) - T \ln w_n^k. \quad (8)$$

In the microscopic definition the smallest value of W_n^k for a fixed n is given by

$$W_{\min}^n(h, T) = 8Jn(1-h) - \max\{4Jk + T \ln(w_n^k), k_{\min}(n) \leq k \leq k_{\max}(n)\}. \quad (9)$$

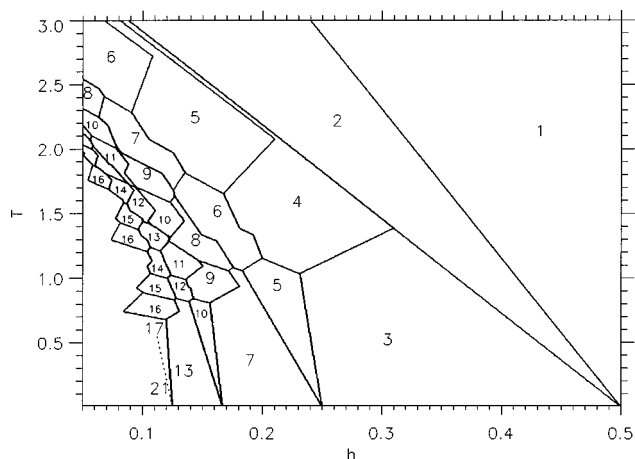


FIG. 2. Domains of constant critical number n_* from the saddle-point definition—see text. Noninteracting clusters are assumed and temperature is measured in the units of J . The boundaries of the 17-spin domain are tentative, and at $T \rightarrow 0$ the domain borders with the one with $n_*=21$, which is indicated by dashed line. The map is formal for higher temperatures where the reduced nucleation barrier is small and cluster interactions cannot be neglected.

A collection of W_{\min}^n for a given pair of h and T represents a “path” as in the left Fig. 1. The largest value of W_{\min}^n on this path

$$W_*(h, T) = \max\{W_{\min}^n(h, T), 1 \leq n \leq n_{\max}\} \quad (10)$$

will determine the nucleation barrier. Currently, the upper bound of $n_{\max}=17$ is available. The value of n with $W_{\min}^n = W_*$ corresponds to the critical number $n_*(h, T)$. Results are shown in Fig. 2. Strictly at $T=0$ and noninteger $1/2h$ the critical size is identical to the one of Ref. 15, but for $T>0$ “secondary”¹⁸ values of the form m^2+1 also appear, with $n_*=17$ being largest available number of this type. The left boundary of the corresponding domain is unknown, except for small T where it borders with $n_*=21$ (dashed line in Fig. 2). For higher T the map of n_* becomes very complex due to a large amount of configurations competing for being the “critical one” with the borders between domains given by straight lines in the h, T coordinates. Nothing special is happening at $T=T_c=J$ multiplied by 2.269, although the neglect of cluster-cluster interactions here is largely unjustified—see Sec. IV—and the results should be treated as formal.

An alternative to the saddle-point definition would be to introduce an average

$$\langle W \rangle_n(h, T) = 8nJ(1-h) - T \ln \sum_{k=k_{\min}(n)}^{k_{\max}(n)} w_n^k e^{4Jk/T} \quad (11)$$

and select a maximum of such values, similarly to Eq. (10):

$$\bar{W}_*(h, T) = \max\{\langle W \rangle_n, 1 \leq n \leq n_{\max}\}. \quad (12)$$

This approach was used to generate a two-dimensional map of n_* in Fig. 3. The situation is simpler compared to the previous definition, but is still very rich, resembling a complicated “phase diagram.” At small T results are identical to the microscopic definition of n_* since only the most compact configurations (for each n) contribute. At higher T other val-

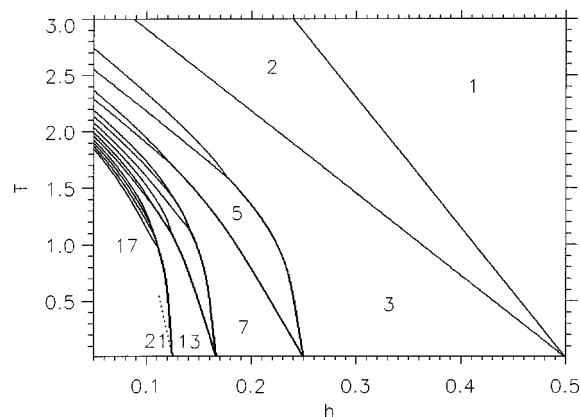


FIG. 3. Same as in Fig. 2, but with an averaged definition of the critical size—see Eq. (12). The narrow unlabeled area extending to $T=0$ between the 7- and the 13-spin domains corresponds to $n_*=10$. The higher-temperature area between the three- and the five-spin domains corresponds to $n_*=4$, the area between the five- and seven-spin domain to $n_*=6$, etc.

ues of the critical size also appear, which is indicated by branching of levels in lower Fig. 3. The dependences on both h and T is monotonic (unlike Fig. 2 where only the h dependence of n_* appears to be monotonic).

C. The “nucleation theorem” and levels of constant nucleation barrier

Within the classical nucleation theory, and if the interfacial tension is independent of supersaturation, the derivative of the barrier with respect to the difference of chemical potentials $\Delta\mu$ determines the critical number:

$$\frac{\partial W_*}{\partial \Delta\mu} = -n_*. \quad (13)$$

Such relations have been used in experimental literature, e.g., Ref. 32 when evaluating n_* from the observed slope of $\ln(I)$, I being the nucleation rate. More recently, see, e.g., Refs. 33–35 a more general validity had been attributed to the above relation, raising its status to that of a nucleation theorem.

In the Ising model the role of $\Delta\mu$ is played by $8Jh$ (this follows from the analogy with lattice gas, e.g., Ref. 18 and references therein). The present treatment does not add new insight into the generality of the theorem since the interfacial tension in the standard Ising model is independent of field. [With any of the above definitions, either in Eq. (9) or in Eq. (11), the h dependence is contained solely in the first term and is linear in h , which immediately leads to Eq. (13)]. However, due to the unusual structure of n_* , it is interesting to observe how Eq. (13) actually works in the present case.

Since n_* is constant in a finite domain of h and T , so is the derivative of the barrier, i.e., the h dependence of the barrier is piecewise linear at any fixed T . At the points where there are multiple values of n_* (as on the boundaries of domains in Figs. 2 and 3, or at the “triple points”) the derivative $\partial W_*/\partial h$ does not exist, or more precisely the barrier has a cusp. With the increase of temperature and/or reduction of field the cusps become more dense. Remarkably, the above properties, as well as Eq. (13) are valid for both the saddle-point and averaged definitions of the critical cluster,

despite the fact that the critical size and the barrier can be quite different in the two cases. In other words, the nucleation theorem does not help in selecting the correct barrier or the critical size, but ensures their consistency with each other.

The temperature derivative is slightly different for the two definitions. In the saddle-point case one has

$$\frac{\partial W_*}{\partial T} = -\ln w_{n_*}^{k_*}, \quad (14)$$

where the asterisk indicates the critical configuration. Again, we note that within the domain of h, T where the same configuration remains critical, the derivative is constant. This, together with Eq. (13) leads to simple expressions for the lines of constant levels of the barrier W_* or of the reduced barrier W_*/T ,

$$\frac{dT}{dh} = -\frac{8Jn_*}{\ln(w_{n_*}^{k_*})}, \quad W_* = \text{const} \quad (15)$$

and

$$\frac{d(\ln T)}{d[\ln E_{n_*}^{k_*}(h)]} = 1, \quad \frac{W_*}{T} = \text{const}. \quad (16)$$

The levels are composed of segments of straight lines. For $W_* = \text{const}$ the lines have the same slope within the h, T domain corresponding to the same critical cluster. For $W_*/T = \text{const}$ the slopes will vary depending on the value of the const.

For the averaged definition one has a somewhat more complex expression

$$\frac{\partial \bar{W}_*}{\partial T} = -S_{n_*}(T), \quad (17)$$

$$S_n(T) = \frac{d}{dT} \left\{ T \ln \sum_{k=k_{\min}(n)}^{k_{\max}(n)} w_{n_*}^{k_*} e^{4Jk/T} \right\}$$

with S_n being an analog of “entropy” for a subsystem containing all clusters with n spins. In Eq. (15) $S_{n_*}(T)$ will replace $\ln(w_{n_*}^{k_*})$ in the denominator. The levels are shown in the top Fig. 4. Since S_1, S_2 , and S_3 are temperature-independent constants, the levels remain straight lines in the corresponding domains (and since $S_1=0$ the lines are vertical in the domain $n_* = 1$). Cusps in the levels coincide with the discontinuities of n_* , in accord with the nucleation theorem, which also accounts for the increase of the density of levels with increasing n_* .

Similarly, for the levels of $\bar{W}_*/T = \text{const} \equiv C$ one can obtain

$$\frac{dT}{dh} = -\frac{8Jn_*}{S_{n_*} + C}. \quad (18)$$

For the domains of $n_* = 1, 2, 3$ levels are straight lines—see the lower Fig. 4.

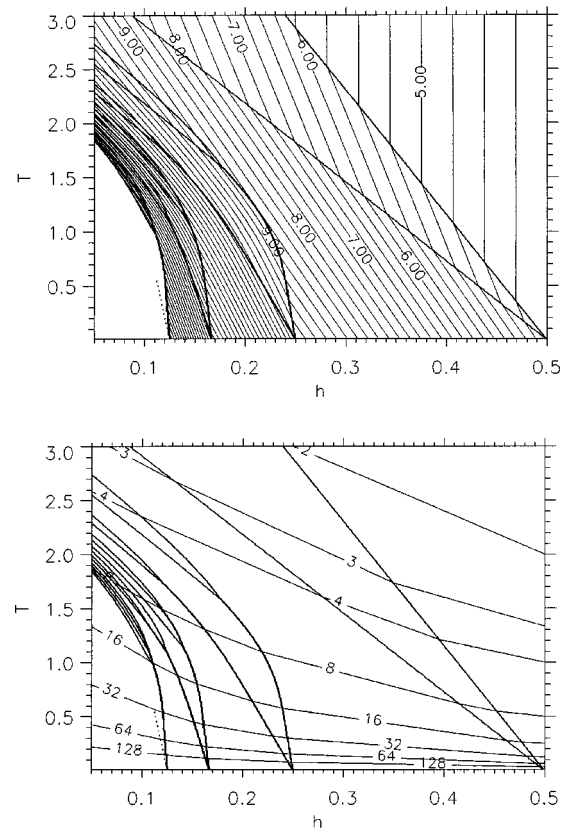


FIG. 4. Levels of constant values of the barrier \bar{W}_* (top figure) and \bar{W}_*/T (bottom figure), superimposed on the domains of constant n_* (as in Fig. 3). The boundaries of those domains determine the cusps in the levels of \bar{W}_* , in accord with the nucleation theorem. Smaller values of \bar{W}_*/T correspond to shorter intervals of steady state nucleation (due to neglected interactions between clusters). In practice, conventional-looking nucleation is expected for $\bar{W}_*/T \geq 8$; for small barriers the results are formal.

D. Upper bound for the nucleation rate

One of the most important applications of the results would be the estimation of the nucleation rate. Strictly speaking, this requires consideration of the dynamics in order to obtain the preexponential. However, some general conclusions can be made if one intends to get only an upper boundary of the rate. In doing so we will employ the electric analogy of Ref. 18 which previously proved efficient in evaluating the lower boundary and in demonstration of the monotonicity of the nucleation rate as a function of h .

In the electric analogy the nucleation flux is treated as an current through a complex network. Cluster configurations of various shapes are “electric junctions,” while the transition rates between each two configurations determine the corresponding resistances (see below). The nucleation rate is the inverse of the total equivalent resistance of the network, R_e^{-1} .

If only the lowest energy paths are considered, after some transformations the network can be made equivalent to a single linear chain¹⁸ with a resistance which exceeds R_e . This gave the lower bound of the rate. When estimating the upper bound, the problem again will be reduced to a linear chain but with a resistance which is *smaller* than R_e . The treatment is directly applicable to the standard nonconserved

dynamics of Refs. 18, 20, and 21 (or, to nonconserved dynamics of Refs. 22 and 23), but can be useful for the less studied Kawasaki dynamics as well.

For simplicity of notations we will keep the n, k labeling (although, in reality there are many distinct shapes with the same n and k). Let $\beta_{n,n+1}^{k,k'}$ be the transition rate from an n, k class to a $n+1, k'$ class. Equivalently, the electric junctions representing those classes are connected by resistors with¹⁸

$$R_{n,n+1}^{k,k'} = (\beta_{n,n+1}^{k,k'} f_n^k)^{-1}. \quad (19)$$

In order to estimate the lower bound on the total equivalent resistance, we will perform several operations each reducing its value. First, all junctions with identical n will be shorted. This turns the network into a series connection of n_{\max} subcircuits, each one with its own resistance R_n^e and with the “true” equivalent resistance of the network $R_e \geq \sum_n R_n^e$. For a fixed n each resistor in the corresponding subcircuit is given by Eq. (19) and is in parallel to other resistors with the same n . The equivalent resistance of the subcircuit is

$$(R_n^e)^{-1} = \sum_{k,k'} 1/R_{n,n+1}^{k,k'}. \quad (20)$$

Next, let us select a maximum for a given n

$$\beta_n^{\max} = \max\{\beta_{n,n+1}^{k,k'}, k, k'\} \quad (21)$$

and replace all $\beta_{n,n+1}^{k,k'}$ by this value. This will reduce every individual resistance (or leave it unchanged), so that

$$R_n^e \geq \left(\beta_n^{\max} \sum_k f_n^k \right)^{-1} = (\beta_n^{\max})^{-1} \exp\{\langle W \rangle_n / T\}. \quad (22)$$

For the total equivalent resistance one thus obtains

$$R_e \equiv I^{-1} \geq \sum_n \frac{1}{\beta_n^{\max}} \exp\left\{ \frac{\langle W \rangle_n}{T} \right\} > \frac{1}{\beta_{n_*}^{\max}} \exp\left\{ \frac{\langle W \rangle_{n_*}}{T} \right\}. \quad (23)$$

As shown in Refs. 20 and 21 once dynamics is specified, the rates $\beta_{n,n+1}^{k,k'}$ can be identified by a computer, which also can select a maximum value. A human (less accurate estimation) can be obtained in the following way, where we restrict ourselves to nonconserved dynamics, such as the Glauber, the Metropolis and the “lattice gas” dynamics discussed in Refs. 18 and 20. Transition rates are the fastest (and simplest) in the lattice gas dynamics, which thus can provide an upper bound of the nucleation rate for the other two. Normalization can be selected in such a manner that $\beta_{n,n+1}^{k,k'}$ will be just equal to the number of sites where a spin can be added in order to convert to the new configuration. This number should not exceed the perimeter P_n^k (we do not discuss here the possibility to fill up “holes” inside clusters, since clusters with holes have a high energy and, at least at moderate T do not have a significant effect on nucleation). The maximum perimeter is $P_n^{k \min(n)} = 2n+2$, so that one has

$$I \leq (2n_* + 2) \exp\left\{ - \frac{\langle W \rangle_{n_*}}{T} \right\}. \quad (24)$$

This is of course an overestimation, which is indicated by the “ \ll ” sign. Typically, only selected sites on the surface of a cluster contribute to transitions and, in addition, the replacement of $\beta_{n,n+1}^{k,k'}$ by its maximum value is definitely excessive and is justified only by the possibility to treat the estimation (23) as a rigorous one. Most likely, the estimation could be substantially improved if the values of $\beta_{n,n+1}^{k,k'}$ were replaced by a maximum selected among the representative configurations with $k=k^*$ and with perimeter closer to that of a compact cluster, but such an intuitive estimation hardly can have a status of an “upper boundary.”

Currently, the lower-boundary estimations of the rate^{18,20,21} are expected to be closer to the actual values, although they are more restrictive in h . The possibility of having the lower and upper bounds for the rate is potentially useful, both from a fundamental point and when predicting the possible outcome of the Monte Carlo simulations.

IV. DISCUSSION

In the present study all cluster configurations with $n \leq 17$ were identified. The results can be used, e.g., when adjusting the preexponential of CNT, as in Ref. 6, only for much larger n . Supposedly, this will substantially improve the accuracy of the description, although an additional study is required here.

Another potential application of the results is verification of standard Monte Carlo (MC) schemes used to describe nucleation and growth. One can check that for $h \leq 0$ (or for small positive h when nucleation still can be neglected and for $n < n_*$), the observed equilibrium distributions are consistent with the exact Boltzmann-type expressions given by Eq. (6).

Once reliable domains of operation for a given MC scheme are identified, one can obtain accurate expressions for the nucleation rate I . Standardization of I suggested earlier (when it tends to 1 in the region of instability, $h > 1$) (Refs. 18 and 20) also can be helpful in order to construct a reliable map of $I(h, T)$ by combined efforts of different groups. Here we remind the reader that so far, even for most common dynamics (Metropolis, Glauber, etc.) there exist no nucleation maps, similar to those in Fig. 4 for the barrier, part of the reason being insufficient reliability of the random number generators or of the entire Monte Carlo schemes for very rare events. (Notably, in many MC simulations the absolute value of I is not reported, but only its exponential part.) Availability of analytical expressions for $I(h, T)$ at small T and moderate-to-high h ,^{18,20,21} as well as numerical results obtained from dedicated MC algorithms,⁷ also will be useful when constructing the “map.”

When identifying the critical cluster, one is reminded that there does not exist an exact definition for either the “critical number” n_* or the “nucleation barrier” W_* . Both quantities have an asymptotic meaning within the framework of the CNT, hence the nonuniqueness of the way in which they can be introduced from the exact equilibrium cluster distributions.

Two possibilities were explored. The first resembles the saddle-point definition of the critical cluster in multidimen-

sional version of CNT, leading to an extremely complicated map of $n_*(h, T)$ as in Fig. 2. The second definition is closer to the one-dimensional version of CNT, when an “average” cluster for each n is constructed, and the critical one is selected among those. The map of $n_*(h, T)$ —Fig. 3—is simpler, but still is very rich. It is worth noting that even consideration of the full dynamic problem does not completely resolve the issue of the critical cluster. As discussed in Refs. 18, 20, and 21 the observable is only the nucleation rate I , while other characteristics, such as the barrier, the preexponential, etc., at least partly depend on conventions.

The complex structure and nonanalyticities of the dependences highlights the potential difficulty of defining a physical “droplet”—a one which would be consistent with the Wulff construction as $h \rightarrow 0$. Most likely, additional averaging over close values of n is required here. Dynamics also is expected to be important since, intuitively, one anticipates that equilibration of a droplet should be faster than transitions between droplets of different sizes.

For the barrier to nucleation only the averaged definition, which is easier for a human to follow, is depicted in Fig. 4. One should keep in mind, however, that depending on the specific dynamics many configurations will not contribute to nucleation, implying a higher barrier or, equivalently a small preexponential of the nucleation rate. For example, at low temperatures many of the lowest energy configurations result in “blind alleys”²¹ and do not contribute to nucleation. It is remarkable, however, that at least within the studied domain of n the optimal paths, as in Fig. 1 are consistent with the standard Metropolis, Glauber, and also with Kawasaki dynamics since on every step the next configuration has either one or two extra bonds, which can be achieved in any of the cases when a single spin is added to a cluster. This means that the barrier to nucleation is estimated reasonably, and specification of the dynamics will have only a moderate effect, mostly altering the preexponential (unless the transition dynamics is itself exponentially slow, as in Refs. 22 and 23).

The usefulness of “thermodynamic” estimations of the barrier, even with overcounting the configurations which contribute to nucleation, is that they can provide one with the upper bound in the estimation of the nucleation rate. This is described in Sec. IV. In addition, having the bottom chart in Fig. 4 is an important reminder of the asymptotic nature of the problem considered, since interaction between clusters is neglected. In reality, after a certain time the nucleated clusters grow so large that they deplete the original pool of down spins, and also can coalesce with each other. Not to add new notations at this stage, we will denote $f_n^k(t)$ the time-dependent kinetic distributions (leaving the original f_n^k for the quasiequilibrium distribution). Within the conventional nucleation picture one requires (e.g., Ref. 18)

$$\sum_{n=1}^{\infty} \left\{ n \sum_{k=k_{\min}(n)}^{k_{\max}(n)} f_n^k(t) \right\} \ll 1. \quad (25)$$

Since this sum will diverge as $t \rightarrow \infty$, there can be only a finite interval of time when the above condition is justified. The steady-state nucleation, as studied in CNT, exists only within this interval, but also after the transient effects are

completed. The corresponding time scales are well separated for $W_*/T \gg 1$, but in practice (say, in the context of Monte Carlo simulations) it can be hard to achieve a separation which is sufficient for an accurate measurement of I . For $W_*/T \gg 8$ the accuracy, somewhat arbitrary, can be considered “reasonable,” although an account for transient nucleation effects can be a substantial improvement.⁸

Another limitation, less connected to the dynamics of a system, is the condition that the subcritical nuclei should be dilute, i.e.,

$$\sum_{n=1}^{n_*} \left\{ n \sum_{k=k_{\min}(n)}^{k_{\max}(n)} f_n^k \right\} \ll 1. \quad (26)$$

This is a weaker limitation than Eq. (25) since only subcritical terms contribute and since for $n < n_*$ one has $f_n^k(t) \approx f_n^k$. Thus, if the condition (26) is valid, there will be a well-defined, though possibly non-steady-state nucleation stage in the system, with interaction between nuclei [indicated by the violation of Eq. (25)] becoming important only after subsequent growth.

Selecting some reasonably small number for the right-hand side of Eq. (26) (e.g., 0.01) would lead to a cusped line, which is not shown in the lower Fig. 4 since it falls above the $W_*/T = 8$ level. An empirical way to test the importance of interactions of subcritical nuclei would be to verify the exponential nature of the h dependence of the number of clusters with a given n .⁶

Finally, in connection with the computer-assisted description of the full nucleation dynamics using symbolic computations^{20,21} one should note that the critical size (at least in its averaged definition), typically, becomes smaller with increasing temperature, as in Fig. 3. This is good news, implying that the amount of configurations which contribute to nucleation, in fact, does not grow as rapidly as suggested by Eq. (7) [with n replaced, e.g., by $n_*(h, 0) + 1$] and that such approaches can be applied to larger T and smaller h than thought before.

V. CONCLUSION

In the present study more than 5×10^8 configurations, representing all possible shapes of clusters with 17 or less spins were identified. Although future increase in computer power will undoubtedly allow one to exceed these numbers, the current values are already large enough to reveal certain patterns in the field and temperature dependences of the critical cluster number n_* and the nucleation barrier W_* . The two latter quantities are related to each other by the nucleation theorem, but otherwise there exists a flexibility in their selection, as long as the nucleation rate I is defined unambiguously. Two major approaches to the definition of n_* and W_* were considered in detail with a rather different structure of the corresponding h, T maps.

ACKNOWLEDGMENT

The authors wish to thank P. A. Rikvold for very useful correspondence.

- ¹M. Volmer and A. Weber, *Z. Phys. Chem., Stoechiom. Verwandtschaftsl.* **119**, 227 (1926); L. Farkas, *ibid.* **125**, 236 (1927); R. Becker and W. Döring, *Ann. Phys. (Paris)* **24**, 719 (1935); Ya. B. Zeldovich, *Acta Physicochim. (USSR)* **18**, 1 (1943); J. Frenkel, *Kinetic Theory of Liquids* (Oxford University Press, Oxford, 1946).
- ²U. Gasser, Eric R. Weeks, A. Schofield, P. N. Pusey, and D. A. Weitz, *Science* **292**, 258 (2001).
- ³K. F. Kelton, G. W. Lee, A. K. Gangopadhyay, R. W. Hyers, T. J. Rathz, J. R. Rogers, M. B. Robinson, and D. S. Robinson, *Phys. Rev. Lett.* **90**, 195504 (2003).
- ⁴E. M. Lifshits and L. P. Pitaevskii, *Physical Kinetics* (Pergamon, New York, 1981), p. 99.
- ⁵S. Auer and D. Frenkel, *Nature (London)* **409**, 1020 (2001).
- ⁶V. A. Shneidman, K. A. Jackson, and K. M. Beatty, *J. Chem. Phys.* **111**, 6932 (1999).
- ⁷M. A. Novotny, in *Computer Simulation Studies in Condensed-Matter Physics XV*, edited by D. P. Landau, S. P. Lewis, and H.-B. Schüttler (Springer, Berlin, 2003), p. 7.
- ⁸V. A. Shneidman, K. A. Jackson, and K. M. Beatty, *Phys. Rev. B* **59**, 3579 (1999).
- ⁹K. Binder and D. Stauffer, *Adv. Phys.* **25**, 343 (1976).
- ¹⁰P. A. Rikvold, H. Tomita, S. Miyashita, and S. W. Sides, *Phys. Rev. E* **49**, 5080 (1994).
- ¹¹M. A. Novotny, P. A. Rikvold, M. Kolesik, D. M. Townsley, and R. A. Ramos, *J. Non-Cryst. Solids* **274**, 356 (2000).
- ¹²E. Stoll, K. Binder, and T. Schneider, *Phys. Rev. B* **6**, 2777 (1972).
- ¹³S. Wonzak, R. Strey, and D. Stauffer, *J. Chem. Phys.* **113**, 1976 (2000).
- ¹⁴V. A. Shneidman and R. K. P. Zia, *Phys. Rev. B* **63**, 085410 (2001).
- ¹⁵E. J. Neves and R. H. Schonmann, *Commun. Math. Phys.* **137**, 209 (1991).
- ¹⁶M. A. Novotny, *Springer Proceeding in Physics: Computer Simulation Studies in Condensed-Matter Physics IX*, edited by D. P. Landau, K. K. Mon, and H.-B. Schüttler (Springer, Berlin, 1997), p. 182.
- ¹⁷A. Bovier and F. Manzo, *J. Stat. Phys.* **107**, 757 (2002).
- ¹⁸V. A. Shneidman, *J. Stat. Phys.* **112**, 293 (2003).
- ¹⁹V. A. Shneidman, *New J. Phys.* (in press).
- ²⁰V. A. Shneidman and G. M. Nita, *Phys. Rev. Lett.* **89**, 025701 (2002).
- ²¹V. A. Shneidman and G. M. Nita, *Phys. Rev. E* **68**, 021605 (2003).
- ²²G. M. Buendia, P. A. Rikvold, K. Park, and M. A. Novotny, *J. Chem. Phys.* **121**, 4193 (2004).
- ²³K. Park, P. A. Rikvold, G. M. Buendia, and M. A. Novotny, *Phys. Rev. Lett.* **92**, 015701 (2004).
- ²⁴V. A. Shneidman, K. A. Jackson, and K. M. Beatty, *J. Cryst. Growth* **212**, 564 (2000).
- ²⁵C. Domb, *Adv. Phys.* **9**, 149 (1960).
- ²⁶M. F. Sykes and M. Glen, *J. Phys. A* **9**, 87 (1976).
- ²⁷S. Redner, *J. Stat. Phys.* **29**, 309 (1982).
- ²⁸J. L. Martin, in *Phase Transitions and Critical Phenomena*, edited by C. Domb and M. S. Green (Academic, New York, 1974), Vol. 3, p. 97.
- ²⁹P. A. Rikvold (private communication). Note in proofs: The data have been posted, see S. Frank, D. E. Roberts, and P. A. Rikvold, e-print: arXiv: cond-mat/0409518 (submitted to *J. Chem. Phys.*).
- ³⁰G. M. Nita, *J. Comput. Phys.* (submitted).
- ³¹G. O. Berim and E. Ruckenstein, *J. Chem. Phys.* **117**, 4542 (2002).
- ³²M. P. Anisimov, V. G. Kostrovskiy, and M. S. Shsteyn, *Heat Transfer-Sov. Res.* **12**, 50 (1980).
- ³³D. Oxtoby and D. Kaschiev, *J. Chem. Phys.* **100**, 7665 (1994).
- ³⁴I. Ford, *Phys. Rev. E* **56**, 5615 (1997).
- ³⁵R. McGrow and D. T. Wu, *J. Chem. Phys.* **118**, 9337 (2003).

The Journal of Chemical Physics is copyrighted by the American Institute of Physics (AIP). Redistribution of journal material is subject to the AIP online journal license and/or AIP copyright. For more information, see <http://ojps.aip.org/jcpof/jcpcr/jsp>